OXFORD UNIVERSITY PRESS | FEMS Microbiology Ecology

http://mc.manuscriptcentral.com/fems

Elevated CO2 induces a bloom of microphytobenthos within a shell gravel mesocosm

Journal:	*FEMS Microbiology Ecology*
Manuscript ID:	FEMSEC-14-12-0663.R1
Manuscript Type:	Research Paper
Date Submitted by the Author:	n/a
Complete List of Authors:	Tait, Karen; Plymouth Marine Laboratory, MLSS Beesley, Amanda; Plymouth Marine Laboratory, MLSS Findlay, Helen; Plymouth Marine Laboratory, MLSS McNeill, Caroline; Plymouth Marine Laboratory, MLSS Widdicombe, Stephen; Plymouth Marine Laboratory, MLSS
Keywords:	Carbon Dioxide Capture and Storage, Sediment, Microphytobenthos, 16S rRNA 454 pyrosequencing, quantitative PCR

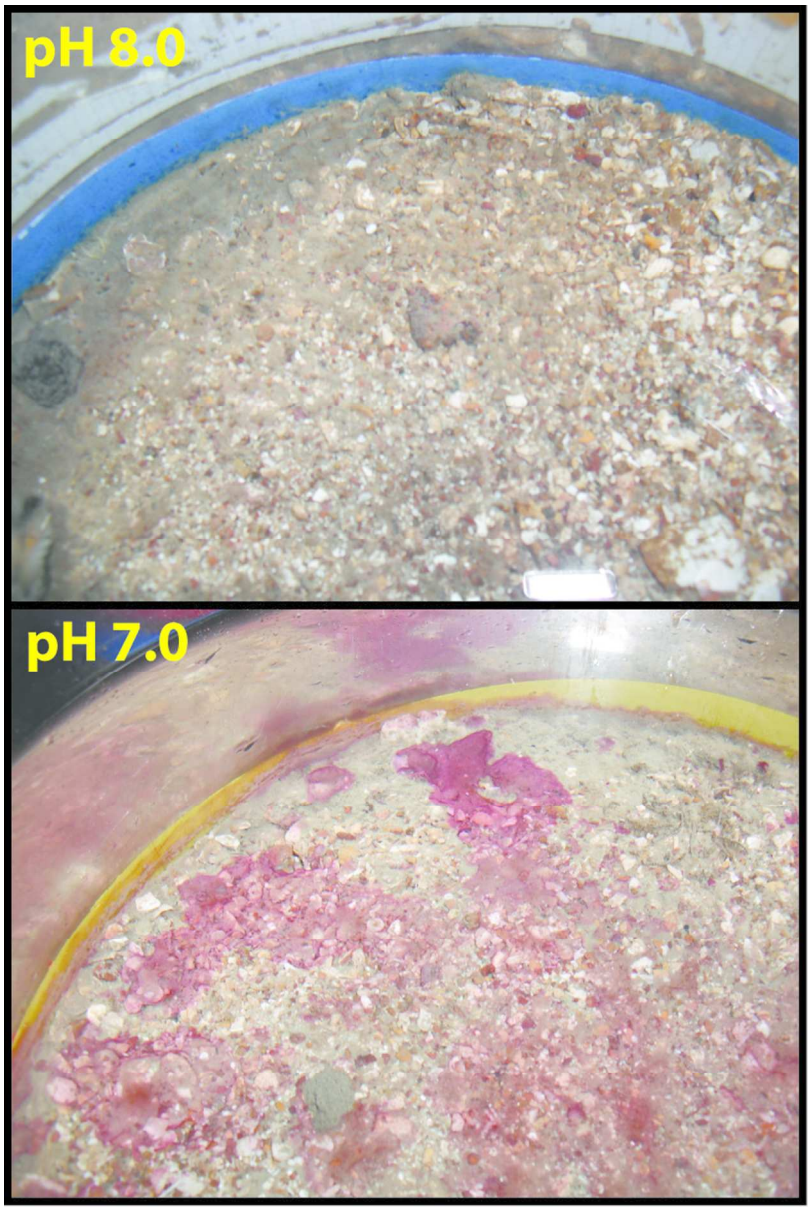

A transient bloom of the cyanobacteria Spirulina sp. together with associated diatoms formed on the surface of sediments exposed to CO2-acidified seawater at pH 7.5 and 7.0, but not at pH 8.0.
69x103mm (300 x 300 DPI)

Elevated CO_2 induces a bloom of microphytobenthos within a shell gravel mesocosm

Karen Tait*, Amanda Beesley, Helen S. Findlay, C. Louise McNeill, Stephen Widdicombe

Plymouth Marine Laboratory, Prospect Place, Plymouth, PL1 3DH, UK

Corresponding Author: Karen Tait, Plymouth Marine Laboratory, Prospect Place, Plymouth, PL1 3DH.

Tel: +44 1752 633415; Fax: +44 1752 633101; ktait@pml.ac.uk

Running title: Elevated CO_2 induces microphytoplankton bloom

Key words: CCS, microphytobenthos, sediment, 16S rRNA 454 pyrosequencing, quantitative PCR, nutrient fluxes

Abstract

The geological storage of carbon dioxide (CO_2) is expected to be an important component of future global carbon emission mitigation, but there is a need to understand the impacts of a CO_2 leak on the marine environment and to develop monitoring protocols for leakage detection. In the present study, sediment cores were exposed to CO_2-acidified seawater at one of five pH levels (8.0, 7.5, 7.0, 6.5 and 6.0) for 10 weeks. A bloom of *Spirulina* sp. and diatoms appeared on sediment surface exposed to pH 7.0 and 7.5 seawater. Quantitative PCR measurements of the abundance of 16S rRNA also indicated an increase to the abundance of microbial 16S rRNA within the pH 7.0 and 7.5 treatments after 10 weeks incubation. More detailed analysis of the microbial communities from the pH 7.0, 7.5 and 8.0 treatments confirmed an increase in the relative abundance of *Spirulina* sp. and *Navicula* sp. sequences, with changes to the relative abundance of major archaeal and bacterial groups also detected within the pH 7.0 treatment. A decreased flux of silicate from the sediment at this pH was also detected. Monitoring for blooms of microphytobenthos may prove useful as an indicator of CO_2 leakage within ~~in~~ coastal areas.

Introduction

Increasing political, social and environmental pressure to alleviate future impacts from global warming and ocean acidification has led many countries to commit to reducing their carbon emissions. One potential mitigation strategy is Carbon Capture and Storage (CCS). This involves the capturing of waste CO_2 from large industries such as coal and natural gas fired power plants, transporting it to a storage site and depositing it underground in geological formations such as depleted oil and gas fields, unmineable coal seams or deep saline formations. CCS technology has the potential to reduce CO_2 emissions from fossil fuel power stations by 80–90% (Holloway, 2007) and the Intergovernmental Panel on Climate Change (IPCC) recognises that effective CCS could play a substantial role in mitigation, potentially reducing CO_2 emissions overall by 21 – 45 % by 2050 (Metz et al, 2005). The development and deployment of technology required for CO_2 capture, transport and storage are making the application of CCS to reduce CO_2 emissions more feasible. Industrial-scale CCS projects are now in operation in Algeria, Norway, Canada and the USA, with many more demonstration and pilot scale ventures in construction globally. The majority of these are on-shore, storing CO_2 within deep saline formations, coal seams and gas fields (Global CCS Insitute, 2012). However, many potential projects are considering off-shore storage, including schemes in Australia, Korea, China, and Italy with several projects aiming to store CO_2 in deep saline formations or abandoned oil and gas fields in the North Sea, including the Netherlands ROAD project, Norways's

Mongstad project and the pilot-level projects in the UK (Global CCS Institute, 2012). Currently, at the Sleipner site in the North Sea, CO_2 from produced gas is directly captured and stored in a subsea aquifer and the Norwegian project Snøhvit, a petroleum production plant in the Barents Sea, is currently capturing CO_2 at their on-shore site and storing off-shore.

Although leakage from storage sites is considered to be unlikely, leakage back up the injection pipe is considered to be a greater risk. If CO_2 leakage did occur from geological storage or pipeline failure, it has the potential to create considerable localised reductions in seawater pH (Blackford et al. 2008; 2009; 2014). Elevated levels of CO_2 can be detrimental to some marine microbes that rely on carbonate structures (Langer et al. 2009; Beaufort et al. 2011), and can also impact microbially-driven biogeochemical nutrient cycling (Hutchins et al. 2007; Fu et al. 2008; Beman et al. 2011; Kitidis et al., 2011). However, only a small number of studies have considered microbial communities and processes within sediments (Ishida et al. 2005; Håvelsrud et al. 2012; Håvelsrud et al. 2013; Ishida et al. 2013; Tait et al., 2013; Tait et al. 2015; Yanagawa et al. 2013; Kerfahi et al. 2014). These studies have reported decreases in microbial diversity (Yanagawa et al. 2013; Kerfahi et al. 2014; Tait et al. 2015), increases to the abundance of bacteria and archaea (Ishida et al. 2005; Ishida et al. 2013), and also possible changes to the degradation of organic matter and biogeochemical cycling of nutrients, including enhanced methane production and sulphate reduction (Ishida et al. 2013; Yanagawa et al. 2013).

Due to their rapid response to environmental changes, a change to microbial activity or community composition could provide an indication of increased pCO_2 or lowered pH. A recent CO_2 release experiment that occurred in the field in Ardmucknish Bay (Oban, Scotland) highlighted the possibility of using microbes and microbial activity as an indicator of CO_2 leaks (Tait et al. 2015). In this instance, a borehole was drilled from shore through the bedrock and into unconsolidated sediments at a location 350 m offshore, and CO_2 gas supplied through a stainless steel pipeline with a gas diffuser welded to the end (11 m below the seabed, which was in turn 12 m below mean sea-level) (Taylor et al. 2015a). A total of 4.2 tonnes of CO_2 were injected into the overlying unconsolidated sediments, but the majority of CO_2 injected *via* the sub-seabed pipe was retained within the sediments. Only ~15 % of the total CO_2 injected was estimated to have been emitted from the seabed in a gaseous phase (Blackford et al. 2014). Bubbles of CO_2 were clearly visible entering the water column and these dissolved rapidly, with measurements of pCO_2 in bottom water at the injection site ranging from 380 to 1500 µatm, depending on injection rate and tidal state (Atamanchuck et al. 2014) and pH measurements within the surface sediments dropped by 0.85 pH

units (Taylor et al. 2015b). Benthic microbes were shown to respond rapidly to the sub-seabed release of CO_2: increases in the abundance of microbial 16S rRNA g^{-1} sediment, used as a proxy for microbial activity, could be detected within the area of active bubble leakage after 14 days of CO_2 release (Tait et al. 2015). There was also evidence that the high CO_2 plume in the water column was advected to a distance of 25 m due to tidal circulation (Atamanchuk et al. 2015), and changes to the abundance of 16S rRNA were also detected at this distance, suggesting that microbes may be highly sensitive to a sub-seabed CO_2 leak. Terminal Restriction Fragment Length Polymorphism (T-RFLP) analysis of the active bacterial community also indicated a rapid shift in composition within areas impacted by the CO_2 release (Blackford et al. 2014). Also evident was a decrease in the abundance of microbial 16S rRNA genes at the leak epicentre during the initial recovery phase that coincided with the highest measurements of DIC within the sediment, but may also be related to the release of potentially toxic metals at this time point (Lichtschalg et al. 2014).

The controlled CO_2 release experiment in Ardmucknish Bay clearly showed that detection of changes to pH or CO_2 may be challenging. Despite the high levels of CO_2 released during the later stages of CO_2 release at the QICS site, pH actually increased as the rise in DIC was buffered by the dissolution of sediment calcium carbonate (Blackford et al. 2014). Different strategies for monitoring potential CO_2 leaks are, therefore, required. The QICS study identified possible microbial indicators for CO_2 leakage within coastal environments; this included an increase in the activity of *Cyanobacteria* and micro-algae, or microphytobenthos during the highest CO_2 release period. Microphytobenthos can be found in the photic zone of marine environments and are composed of microalgae, predominantly *Baccillariophyceae*, but *Chlorophyceae* and *Dinophyceae* can also be present, and bacteria including *Cyanobacteria*, heterotrophic bacteria, chemolithotrophic bacteria, anoxygenic phototrophs and sulphate-reducing bacteria (Paterson & Hagerthey, 2001; Hubas et al. 2011). These microbes accumulate at the sediment surface and exhibit high rates of photosynthesis, contributing up to 50% of estuarine primary production (Underwood and Kromkamp, 1999), and fuelling much of the secondary production within these ecosystems (Middleburg et al, 2000).

In the present study, fifty cores containing carbonate rich gravel collected from the Eddystone reef in the Western English Channel (50° 11.55 N, 04° 17.0 W) during September 2010 were incubated using seawater adjusted to five different CO_2 concentrations by bubbling with pure CO_2, the flow of which was monitored *via* an electronic feedback system. Twenty five sediment cores were incubated for a period of 2 weeks and the remainder for 10 weeks. The aim of the experiment was to examine the impact of a CO_2 leak on meio- and macrofauna residing within the sediments. However, during

the course of the experiment, a pink microphytobenthos mat appeared on top of the cores exposed to seawater adjusted to pH 7.0 and 7.5, providing the opportunity to identify key microbial species responding to elevated CO_2 levels. Surface sediment samples were taken for microbial analyses, the *Cyanobacteria* and micro-algae resident within the mat were identified, and the abundance of *Cyanobacteria* and micro-algae within the different pH treatments compared at two and ten weeks. This was followed by a detailed analysis of the microbial community present at week ten in cores receiving ambient pH seawater, and seawater adjusted to pH 7.0 and 7.5. After a two and ten week incubation period, measurements were made of the flux of nutrients from the sediment to the water column.

Materials and Methods

Mesocosm set-up

Carbonate rich gravel was collected on the 15th September 2010 from the Eddystone reef in the Western English Channel (50° 11.55 N, 04° 17.0 W). Sediment was collected using a 0.1 m^2 boxcorer and used to fill 50 clear Perspex cores (19 cm diameter, 40 cm deep) to a depth of 30 cm and topped off with seawater (10 cm depth) to prevent desiccation and minimise temperature change. Cores were transferred to the seawater acidification facility located in the mesocosm of the Plymouth Marine Laboratory (PML), UK. Once at PML the cores were continuously supplied with natural seawater collected from the Eddystone reef site (temperature ≈11 °C, salinity ≈ 34) at a rate of 15 mL min^{-1} for a period of 6 days to allow both the fauna and biogeochemical profiles within the cores to recover.

The Ardmucknish Bay experiments indicated the CO_2 was emitted from the sediment as gas bubbles that rapidly dissolved, reducing the pH in the sediment/water boundary layer (Taylor et al. 2015b). Within this experiment, the 50 cores were randomly allocated to 1 of 5 pH treatment levels (8.0 [control], 7.5, 7.0, 6.5 and 6.0) and supplied with unfiltered seawater from one of five header tanks at a rate of approximately 15 mL min^{-1}. Seawater for the header tanks was collected from the Western English Channel Observatory long term monitoring site L4 (50° 15.00' N, 4° 13.02' W). The seawater in each of the pH 7.5, 7.0, 6.5 and 6.0 header tanks was maintained at the desired pH by bubbling with pure CO_2, following the methodology of Widdicombe and Needham (2007). No additional CO_2 was added to the pH 8.0 tank. The temperature within the mesocosm was maintained at 11 °C, with a light: dark cycle of 16 h: 8 h. The water within each of the reservoir tanks and sediment cores was monitored three times per week for temperature, salinity (WTW LF187

combination temperature and salinity probe), and pH (Metrohm, 826 pH mobile with a Metrohm glass electrode, calibrated to NBS). Water samples were taken once a week to determine total alkalinity (TA) and nutrient concentrations. Nutrients were analysed with an autoanalyser (Brann & Luebbe Ltd., AAIII) using standard methods (Brewer & Riley, 1965; Grasshoff, 1976; Kirkwood, 1989; Mantoura & Woodward, 1983; Zhang & Chi, 2002). Alkalinity was measured by poisoning 100 mL water samples with $HgCl_2$ according to Dickson et al. (2007) then analysing via potentiometric titration using an Alkalinity Titrator (Apollo SciTech Model AS-ALK2) and using Batch 100 certified reference materials from Andrew Dickson. Using pH, TA, temperature, salinity, phosphate and silicate, the other carbonate parameters (dissolved inorganic carbon (DIC), pCO_2, calcite and aragonite saturation states~~, etc.~~) were calculated using the CO2SYS programme (Pierrot et al. 2006) using constants from Mehrbach et al. (1973) refitted by Dickson and Millero (1987) and the KSO_4 dissociation constant from Dickson (1990).

Two weeks after the start of the exposure (5th – 6th October 2011), five cores from each pH treatment (25 cores in total) were randomly selected and sampled for measurements of sediment nutrient flux, microbial abundance and community structure (described below) and then destructively sampled for meiofauna and macrofauna analysis (to be reported elsewhere). The remaining 25 cores were allowed to run for an additional 8 weeks before being similarly sampled (29th – 30th November 2011).

Sediment nutrient flux

From each core, water samples were taken from the overlying 10 cm of water to determine the rate of sediment flux for five nutrient species (nitrate, nitrite, ammonium, silicate and phosphate). Over two consecutive days, three 50mL water samples were drawn from each core, filtered through a 47mm ø GF/F filter into an acid washed Nalgene bottle and immediately frozen. In addition to these "core water" samples, five "inflow water" samples were taken from each of the five header tanks. These samples were also filtered and then frozen and analysed as described above for nutrient monitoring. Sediment fluxes were calculated using the equation:

$$F_x = \left(\frac{C_i - C_0}{A}\right) \cdot Q \qquad \text{(Eq. 1)}$$

where F_x is the flux of nutrient x (µmol m^{-2} h^{-1}), C_i is the mean concentration of nutrient x in the inflow water (µM), C_0 is the mean concentration of nutrient x in the water above the sediment in the experiment cores (µM), Q is the rate of water flow through the core (L h^{-1}) and A is the area of the core (m^2) (Widdicombe and Needham, 2007).

Identification of Cyanobacteria *and micro-algae community within the pink microphytobenthos mat*

During week 6, small sections of the pink microphytobenthos mat were removed from the surface of the pH 7.0 and 7.5 cores ~~at week 7~~ with a sterile scalpel and washed gently with filter-sterilised pH 7.0 or pH 7.5 seawater to remove sediment material. A light microscope (Reichert Jung Polyvar) and an Optronics Magna Fire SP camera was used to image small sections of the material. DNA was extracted from six small sections (0.2g) of the pink mat using the PowerBiofilm™ DNA Isolation Kit (MoBio Laboratories) according to the manufacturer's instructions. To taxonomically identify the cyanobacteria and algae present within the pink mat, PCR amplification of 16S rRNA gene fragments was performed using the PCR primer pair CYA-359F (5' GGGGAATYTTCCGCAATGGG-3') and CYA-781R (5'-GACTACWGGGGTATCTAATCCCW-3'), which are specific for *Cyanobacteria* and micro-algae chloroplast (Nübel et al., 1997), using the PCR conditions described in Tait et al. (2015). This was done in triplicate for each of the six DNA extractions and the PCR products cloned and transformed using the pGEM-T Easy Vector System II cloning kit (Promega) according to the manufacturer's instructions. Clone libraries were also made from DNA extracts of the day 0 samples to determine the initial composition of the microphytobenthos community. Sequences were clustered into Operational Taxonomic Units (OTUs) based on 97 % sequence similarity using Uclust (using the QIIME (Quantitative Insights into Molecular Ecology) pipeline; Caporaso et al. 2010). To assign taxonomy to each OTU, a representative sequence from each OTU cluster was chosen, the representative sequences aligned using PYNAST, and taxonomy assigned by comparison with the Greengenes (version Feb 2011) (Pruesse et al. 2007) and the NCBI databases.

RNA extraction from sediments

After 2 and 10 weeks incubation, 8 small sediment samples (approx. 0.5 g each) were taken from across the sediment surface (top 0.5 cm) in order to determine the composition of the active microbial community. The eight samples from each core were combined and homogenised, placed into 50 mL Falcon tubes, mixed with a sterile spatula and immediately frozen (-80 °C). This was compared to samples taken in a similar manner at the start of the experiment (day 0). RNA was extracted from 2 g of sediment using the MoBio RNA Powersoil Total RNA Isolation Kit (MoBio Laboratories) according to the manufacturer's instructions.

cDNA synthesis and RT-qPCR

The RNA was reverse transcribed using the QuantiTect Reverse Transcription Kit (Qiagen) with 1 µL of RNA and the supplied random primers. An ABI 7000 sequence detection system (Applied Biosystems, Foster City, USA) and QuantiFast SYBR Green PCR Kit (Qiagen) was used for all qPCR

measurements. For each sediment sample, 1 µL of cDNA was used to determine the abundance of cyanobacterial 16S rRNA using CYA359F and CYA781R and bacterial 16S rRNA using Bact1369F (CGGTGAATACGTTCYCGG) and Prok1492R (GGWTACCTTGTTACGACTT) (Suzuki et al. 2000) following the methodology described in Tait et al. (2015). The 20 µL reaction mixture contained 10 µl of Master Mix and 300 nM of each primer, and PCR conditions were 5 min at 95 °C followed by 40 cycles of 95 °C for 15 s, 52 °C for 30 s and 72 °C for 45 s. Standard curves were produced from cDNA following prior *in vitro* transcription of cloned sequences using the Ampliscribe T7 Flash kit (Epicentre) following methodologies described by Smith et al. (2006). 16S rRNA abundance was quantified via comparison to standard curves using the ABI Prism 7000 detection software. Automatic analysis settings were used to determine the threshold cycle (CT) values and baselines settings. The no-template controls were below the threshold in all experiments. For each standard curve, the slope, y intercept, co-efficient of determination (r^2) and the efficiency of amplification was determined as follows: *Cyanobacteria*/chloroplast 16S rRNA: r^2 = 0.993, *y* intercept = 36.48, *E* = 94.5 %; bacterial 16S rRNA r^2 = 0.997, *y* intercept = 35.05, *E* = 96.3 %.

16S rRNA 454 pyrosequencing and analysis

An opportunity arose to have a small number of the sediment core samples analysed using 16S rRNA tagged 454 pyrosequencing. Twelve cDNA samples (see above) were chosen: 4 replicate cores from the pH 8.0, pH 7.5 and pH 7.0 treatments. These pH treatments were selected because of the presence of the pink mat, but also because the data would also be useful for studies of the impact of ocean acidification on sediment microbial communities. Possible changes to both bacterial and archaeal community composition was examined. For bacteria, cDNA was amplified with the V4-V5 region of 16S rRNA using the PCR primers 518F (equal quantities of CCAGCAGCCGCGGTAAN and CCAGCAGCTGCGGTAAN) and 926R (equal quantities of CCGTCAATTCNTTTRAGT, CCGTCAATTCTTTTGAGT and CCGTCAATTTCTTTGAGT) (Huse et al. 2010). For archaea, the PCR primers Parch519F (CAGCCGCCGCGGTAA) and ARC915R (GTGCTCCCCCGCCAATTCCT) (Coolen et al. 2004) were used. The 30 µl-volume reaction mixtures contained 1 µl of cDNA, 5X PCR buffer (Promega), 2.5 mM $MgCl_2$, 0.1 mM dNTPs, 1.5 U of GoTaq Hot Start DNA polymerase (Promega) and 0.6 µM of forward and reverse primers. PCRs were initially denatured for 3 mins at 94 °C, followed by 20 cycles of 94 °C for 30 secs; primer annealing at 57 °C for 45 secs, and elongation at 72 °C for 60 secs. A final elongation step was performed at 72 °C for 5 min. A final 5 cycles were performed in a subsequent PCR reaction containing 1 µL PCR product and primer sets modified with an 8 bp multiplexing identifier (MID) adaptor used for barcode tagging, thereby allowing for post-sequencing separation of the samples, using the above PCR conditions. Each sediment sample was amplified in

triplicate, the triplicates pooled, cleaned using the Agencourt AMPure XP Purification System (Beckman Coulter, Bromley, UK) and the concentration of each product calculated using the PicoGreen assay (Invitrogen) against standard DNA curves with $r^2 \geq 0.99$. DNA libraries were prepared for sequencing using the Roche emPCR Method Manual – Lib-L MV and the Roche Sequencing Method Manual for the GS FLX Titanium Series. Picotitre plates were used with an 8 lane gasket. Data was processed using QIIME (Caporaso et al. 2010). Sequences were first de-multiplexed, denoised and chimeras removed using Ampliconnoise (Quince et al. 2011), and clustered at 97 % sequence similarity using Uclust. Representative sequences were PYNAST aligned and taxonomy assigned using the Silva database version 108 (Pruesse et al. 2007). This assigned 87.7 % of bacterial sequences and 87.2 % archaeal sequences to Order level. Sequence data is available at the EMBL database (accession number ERP002371).

A total of 109582 high quality sequences were obtained for the 12 sediment cores examined, ranging from 5237 to 15424 per sample with an average read length across all samples of 375 bp (Supplementary Table 1). The ratio of archaeal:bacterial sequences obtained from each core was similar to the values obtained from the qPCR (Supplementary Table 1), and so the archaeal and bacterial data-sets were combined, OTUs picked at 97% sequence similarity and the data set randomly sub-sampled so each sample contained the same number of sequences (5237).

Statistics

For qPCR data (Figure 3), all error bars are standard deviation (n = 5). Two-way ANOVA was used to test for differences in the quantity of 16S rRNA copy numbers followed by post-hoc tests to identify pH treatments with significantly different abundances. For the 16S rRNA tagged 454 pyrosequencing data set the Qiime pipeline and Primer vs 6.1 multivariate analysis software (Clarke and Gorley, 2006) were used to calculate alpha diversity for each clone library. Resemblances between samples were generated using the Bray-Curtis coefficient, calculated using both the abundance and the presence and absence of OTUs. Non-metric multidimensional scaling (MDS) was applied to assess the grouping structure of samples and their corresponding pH treatment. An analysis of similarity (ANOSIM) was used to determine the effect of pH on community composition.

Results

Measurements of environmental parameters

pH remained relatively stable throughout the 10 weeks, with a maximum standard deviation of 0.3 pH (across cores) found at the lower pH conditions (Table 1). Temperature and salinity remained constant varying by an average of 0.6 ºC and 0.47, respectively (Table 1). Total alkalinity was more variable between the cores, resulting in relatively high standard deviations for each treatment, however, there was no significant differences between treatments. The low pH and high alkalinity values resulted in high carbon conditions (see pCO_2 and DIC values in Table 1), and the saturation state for aragonite was near or below 1 in all cores below pH 7.5 (Table 1). Also shown are nutrient concentrations: there were no differences between treatments for each nutrient measured.

pH impact on the flux of silicate from the sediment to the water column

Although there was a shift in the flux of dissolved inorganic nitrogen (DIN) through the course of the experiment, going from a source at week 2 to a sink at week 10 (results not shown), with the exception of silicate (Figure 1), there was no significant relationship between pH and the flux of nutrients (ammonia, nitrate, nitrite or phosphate) measured over a 24 h period after 2 and 10 weeks incubation (results not shown). There was a positive flux for silicate at week 2 and week 10. pH had no impact on silicate flux at week 2 (one-way ANOVA $F = 0.12$; $p = 0.972$) (results not shown), but there was a significant decrease in the flux of silicate from the sediment to the water column in the pH 7.0 and 7.5 treatments when compared to the other treatments (one-way ANOVA $F = 3.24$; $p = 0.033$) (Figure 1).

Identification of the composition of the microphytobenthos mat

The pink-pigmented mat appeared in cores receiving seawater adjusted to pH 7.0 and 7.5 after five weeks incubation, peaked at eight weeks (Figure 2A), but was still visible in small patches after ten weeks in the cores exposed to pH 7.0 seawater. No pink colouration was evident on sediment cores receiving ambient pH seawater (Figure 2B), or cores receiving seawater adjusted to pH 6.0 and 6.5. Examination under a microscope revealed the presence of a community mainly comprising pink filamentous *Cyanobacteria* and diatoms (Figure 2C). From the microscope analysis, the same community appeared to be present within all samples analysed from both pH 7.0 and pH 7.5 cores. Analysis of sequence data obtained from clone libraries of PCR-amplified *Cyanobacteria* and chloroplast 16S rRNA gene sequences revealed the *Cyanobacteria* to be *Spirulina* sp., and diatoms of the Orders *Naviculales* (OTUs 1) and *Bacillariales* (OTUs 2 and 3) (Figure 2D). No other cyanobacterium other than *Spirulina* was detected in the clone library. OTU 1, most closely related to a *Navicula* sp., was the most abundant diatom detected (50% of sequences). Although OTUs 1, 2 and 3 could be detected in samples taken on day 0, no *Spirulina* sp. sequences were detected,

suggesting that this particular species may have colonised the shell gravel from the seawater overlying the sediment cores in the mesocosm.

pH impacts on the abundance of 16S rRNA

The activity of *Cyanobacteria* and micro-algae within the different treatments was compared using qPCR. Measurements with PCR primers specific for *Cyanobacteria* and chloroplast 16S rRNA revealed both significant changes with pH treatment and when the week 2 and week 10 measurements were compared, but differences in the pH response at week 2 and weeks 10 were also evident (Figure 3A). At week 2, *Cyanobacteria* 16S rRNA abundance increased in the pH 6.5, 7.0 and 7.5 treatments, but the abundance in the pH 6.0 was not significantly different to the value in the control sediments. At week 10, increases in 16S rRNA abundance were evident only in the pH 7.0 and 7.5 treatments and was equivalent to an 295% and 690% increase in abundance of cyanobacterial 16S rRNA, respectively, when compared to the pH 8.0 treatments. This is indicative of a substantial increase in the activity of *Cyanobacteria* and micro-algae within the pH 7.0 and pH 7.5 treatments. Similar profiles were evident for measurements of bacterial 16S rRNA (Figure 3B).

Detailed comparison of the microbial community structure within the pH 7.0, pH 7.5 and pH 8.0 treatments

Although the number of OTUs and measures of species richness (Figure 4A) did not differ between pH treatments, there was a significant drop for measurements of Shannon diversity (Figure 4B) and Pielou eveness (Figure 4C) within the pH 7.0 treatments (one-way ANOVA $F = 7.39$; $p = 0.013$ and $F = 8.24$; $p = 0.009$, respectively). This suggests that although the same OTUs were present in all treatments, the low pH cores may have become numerically dominated by a small subset of OTUs. To compare community composition within the different sediment cores, resemblence matrices were generated using the Bray-Curtis coefficient, calculated using both the abundance and also the presence/absence of OTUs. Bray-Curtis abundance matrices indicated significant differences between pH treatments (ANOSIM $R = 0.274$; $p = 0.035$), whereas the resemblance matrices generated using the presence/absence data sets indicated no differences between treatments (ANOSIM $R = 0.009$; $p = 0.143$), confirming that the changes in community structure were driven by changes in the relative abundances of OTUs rather than by the presence or absence of different OTUs in each of the pH treatments. Multidimensional scaling ordination analysis revealed considerable overlap between the structure of the microbial communities from the pH 8.0 and pH 7.5 treatments, but that the pH 7.0-treated cores differed (Figure 5A). Post-hoc tests confirmed the pH 7.0 treatments were significantly different to the pH 8.0 and pH 7.5 cores (comparisons of pH 7.0

and 7.5 R = 0.354, p = 0.029; pH 7.0 and pH 8.0 R = 0.521, p = 0.029; pH 7.5 and pH 8.0 R = -0.094, p = 0.657). Together, this suggests that there were key changes to the relative abundance of dominant OTUs within the pH 7.0-treated cores, and that there may have been phylogenetic structure to these changes.

When the OTUs were grouped at Class-level taxonomy, nine Classes were seen to have abundances greater than 2 % within the data-set (in order of most abundant: Chloroplasts, Subsection III of the *Cyanobacteria*, *Alphaproteobacteria*, *Gammaproteobacteria*, *Deltaproteobacteria*, Marine Group I (*Thaumarchaeota*), the *Planctomycete* Classes OM190 and *Planctomycetia* and the *Gemmatimonadetes*). Of these nine, five showed significant increases or decreases within the pH 7.0 cores (Figure 5B). The relative abundance of chloroplast and *Cyanobacteria* Sub-section III sequences more than doubled at pH 7.0 when compared to the pH 8.0 and pH 7.5 treatments. In contrast, the *Alphaproteobacteria*, *Planctomycetes* Class OM190 and the *Thaumarchaeota* Marine Group I all decreased with decreasing pH (Figure 5B). When these differences were examined in more detail, the changes to the relative abundance of the Classes Chloroplast, Subsection III and Marine Group I were mainly due to changes in the relative abundance of single OTUs (Figure 5C). For Subsection III, the relative abundance of an OTU most closely related to *Spirulina* sp. and within the Chloroplasts, an unidentified diatom (OTU #5248), closely related to OTU 1 (*Navicula* sp.) identified in Figure 2D, both increased in abundance within the pH 7.0 treatments. An uncultured *Nitrosopumilus* (OTU #7731) was mostly responsible for the decreases in relative abundance seen for the Marine Group I Class. These OTUs were first, second and fourth most abundant OTUs within the entire data-set. The third most abundant, OTU #4558, very similar to the diatom most closely related to *Psammodictyon panduriforme* (OTU 3) identified in Figure 2D, did not differ with pH (results not shown). The fifth most abundant OTU belonged to the *Rhodospirillales*. Although the relative abundance of this particular OTU did not differ between pH treatments (Figure 5C), the changes to the Alphaproteobacteria could be traced to a decrease in the relative abundance of members of the family *Rhodospirrillaceae*. There were significant decreases in the relative abundance of this family in both the pH 7.0 and 7.5 treatments when compared to the pH 8.0 cores (one-way ANOVA F = 9.43; p = 0.006).

Discussion

This mesocosm study clearly demonstrated that a CO_2-induced decrease in the pH of seawater to either 7.5 or 7.0 resulted in a transient bloom of benthic *Cyanobacteria* and diatoms, predominantly consisting of the cyanobacterium *Spirulina* sp. and diatom species (Figures 2 and 5). Although the

bloom appeared visually to have begun to die back by week 10 of the experiment, qPCR measurements of 16S rRNA specific for *Cyanobacteria* (Figure 3) and detailed analysis of the community composition indicated increased abundance of the *Spirulina* sp. and a diatom most closely related to *Navicula* sp. within the pH 7.0 treatments (Figures 5c). Also evident were changes to the composition of the active bacterial and archaeal community, including decreases to the relative abundance of *Rhodospirillales*, *Planctomycetes* Class OM190 and *Thaumarchaeota* (Figure 5). A decrease in the flux of silicate from the sediment to the water column under these pH conditions was also evident (Figure 1), perhaps indicating increased uptake of silicate by diatoms to support growth and reproduction, or due to the increased adsorption of silicate onto hydrated metal oxides. This is known to occur within sediments under the oxic conditions brought about by the activity of microphytobenthos (Hartikainen et al. 1996).

Although the diatom species could be detected within pre-exposure sediments, it is possible that the *Spirulina* sp. was introduced from the overlying seawater used to feed the sediment cores within different concentrations of CO_2. The composition of microphytobenthos has been shown to vary with sediment type. Although they are predominantly composed of diatoms, previous studies have recorded high incidences of *Cyanobacteria* on coarse grain sediments (Waterman et al. 1999), and Franks and Stolz (2009) showed that newly colonised sands were mainly comprised of *Oscillatoria* sp. and *Spirulina* sp., indicating that this species readily colonised coarse grain sediments such as those used within this experiment. Experiments designed to trial the efficiency of *Spirulina* sp. for CO_2 sequestration have also shown this cyanobacterium to increase biomass and CO_2 fixation rates within photobioreactors receiving 6 % CO_2 (de Rosa et al. 2011), suggesting that members of this Genus are well-equipped to thrive under elevated CO_2 conditions.

Studies of the impact of elevated CO_2 on *Cyanobacteria* within biofilm communities have shown members of the Chroococcales to increase in abundance (Russell et al. 2013; Taylor et al. 2014), and enhance inorganic uptake and growth for a number of phytoplankton groups, including the *Cyanobacteria Trichodesmium* (Hutchins et al. 2007; Levitan et al. 2007; Lomas et al. 2012) and diatoms (e.g. Tortell et al. 2008; Trimborn et al. 2009; Sun et al. 2011). Both the *Spirulina* sp. and *Navicula* sp. increased in abundance within the pH 7.0 and 7.5 treatments, and these were presumably responding to an increase in pCO_2 concentration. However, the relative abundance of the OTU most closely related to *Psammodictyon panduriforme* did not differ between the pH treatments (Figure 5). This difference may be, in part, related to the carbon concentrating mechanisms (CCMs) used by marine *Cyanobacteria* and micro-algae. Due to the inefficiencies of the

key carbon fixing enzyme, RubisCO (ribulose-1,5-bisphosphate carboxylase/oxygenase), many phytoplankton species, including diatoms and *Cyanobacteria* have evolved CCMs to elevate intracellular concentrations of CO_2, but at an energy cost (reviewed by Reinfelder, 2011). It has been suggested that phytoplankton that rely on diffusive entry of CO_2 or those that are able to suppress their CCMs may have a selective advantage under elevated CO_2 conditions (Raven, 1991). Laboratory studies have indicated that many diatoms possess relatively efficient CCMs that are strongly regulated by CO_2 concentration (Burkhardt et al. 2001; Rost et al. 2003; Trimborn et al. 2009; Hopkinson et al. 2011). However, diatoms utilise a high diversity of methods to acquire carbon (Reinfelder et al. 2011), and so species specific responses to elevated levels of CO_2 may be detected (Kim et al. 2006; Trimborn et al. 2009; Torstensson et al. 2012). Our results are similar to the response of the pelagic mesocosm of Kim et al. (2006) where an increase in the specific growth rate of *Skeletonema costatum* was observed at 750 µatm CO_2, but there was no effect on the growth rate of *Nitzschia* spp.

Alternatively, the lack of response of the *Psammodictyon* sp. may have been due to pH changes brought about by the decrease in pH rather than an increase in CO_2 concentration. Several diatom taxa have a statistically significant relationship with pH, and this has been exploited in the use of diatom community composition as an ecological indicator for monitoring environmental change in lakes, and to reconstruct past lake-water pH (Birks et al. 1990). In a review of literature published on the effects of pH on marine phytoplankton growth under laboratory conditions, some species were able to grow at a wide range of pH, whereas others had growth rates that varied greatly over a 0.5 to 1.0 pH unit change: pH can inhibit growth regardless of CO_2 concentration for some phytoplankton species (Hinga 2002).

The presence of microphytobenthos has been shown to increase the lability of sediment organic matter and as a result, increase bacterial abundance (Hardison et al. 2013). This would be expected to alter the activity of archaea and bacteria within the sediment surface. Within this study, we have shown that in conjunction to the increase to the *Spirulina* sp. and *Navicula* sp., there was a corresponding decrease in the relative abundance of 16S rRNA sequences most closely related to the Alphaproteobacteria (which could be traced to a decrease in the Family *Rhodospirrillaceae*), the Planctomycete Class OM190 and the *Thaumarchaeota* Marine Group I (Figure 5c). The decrease to the *Thaumarchaetoa* was mainly due to the decrease in the relative abundance of a single *Nitrosopumilus* sp. (Figure 5). These archaea are known aerobic ammonia oxidisers, converting ammonia to nitrite. However, it is known that pH treatment had no impact on ammonia oxidising

within this mesocosm experiment: Kitidis et al. (2011) reported no differences to ammonia oxidising rates between pH treatments. However, ammonia oxidising bacteria may also have been present: the relative contribution of bacteria and archaea to nitrification within these sediments is not known. While some archaeal ammonia oxidisers can tolerate a wide range of oxygen levels, others appear to be more suited to low-oxygen environments (Erguder et al. 2009). It may be possible that the archaeal ammonium oxidisers present within the sediments within this study preferred lowered oxygen concentrations and were sensitive to the presumably high levels of oxygen produced by the photosynthetic activities of the dominant *Cyanobacteria* and diatom species. The *Rhodospirrillaceae* contain the purple non-sulphur bacteria, common inhabitants of microphytobenthos mats. This group of bacteria are anaerobic anoxygenic phototrophs, typically using hydrogen as a reducing agent during photosynthesis (Hubas et al. 2011). The purple non-sulphur bacteria migrate away from oxygen (Hubas et al. 2011), and it is also possible that the high levels of oxygen presumably produced by the photosynthetic activity of *Cyanobacteria* and diatoms within the biofilm resulted in a decrease in this group. Members of the OM190 have been detected in a variety of marine environments, and are commonly found associated with algae (Rappe et al., 1997; Bengston & Ovreas, 2010). But as no cultured representative of this deeply branching group currently exists, there is very little knowledge on the function of this group within marine ecosystems. Interestingly, the relative abundance of the class *Planctomycetacia* was shown to increase with increasing pCO_2 concentration in a previous benthic mesocosm studying the impact of elevated pCO_2 on Arctic sediment microbial communities (Tait et al. 2013). More information is required on the function of the members of the *Planctomycetes* within marine sediments to understand the impact of elevated CO_2 on this group, and the possible consequences for the biogeochemical cycling on nutrients within marine sediments.

The microphytobenthos bloom was most evident in the pH 7.0 and 7.5 cores after 6 weeks, peaked at 8 weeks but had declined by week 10, being only visible in small patches in the pH 7.0 cores. The dense layer of diatoms and *Cyanobacteria* at the sediment surface may have depleted essential nutrients, causing a crash in the microphytobenthos population. Alternatively, an increase in grazing by meiofauna may have resulted in the decrease in microphytobenthos. Microphytobenthos are an important food source for meiofauna in intertidal environments (Miller et al., 1996). Although acidification did not change meiofauna abundance in the pH 7.0 or 7.5 treatments when compared to the pH 8.0 controls (Jeroen Ingels, personal communication), a number of studies have now shown that many invertebrates cope with elevated CO_2 by use of energetically expensive

physiological processes (Findlay et al. 2010; Stumpp et al. 2012) and as a result may consume more food per individual (Thomsen et al. 2013).

There was a significant increase in the abundance of cyanobacterial 16S rRNA within the pH 6.5 cores at week 2, but at week 10 the abundance of cyanobacterial 16S rRNA within both the pH 6.0 and 6.5 treatments did not differ to the pH 8.0 cores (Figure 3). Although there was a shift in the flux of DIN through the course of the experiment, going from a source at week 2 to a sink at week 10, there were no significant differences between pH treatments for both DIN and dissolved inorganic phosphate fluxes. The levels of nutrients measured within the seawater above the cores also indicated that there were no differences to the nutrient concentrations with pH (Table 1), and so it is unlikely that the pH 6.0 and 6.5 cores were nutrient limited. Again, this may have been due to increased grazing by meiobenthos under the high CO_2 conditions. Alternatively, it is conceivable that the CO_2-induced low pH directly impacted the growth of microphytobenthos bloom within the pH 6.0 and 6.5 treatments. Although both *Spirulina* sp. and diatoms are capable of growing at a range of pH, including < pH 6.0 for certain species in laboratory cultures (Ramanan et al. 2010; Hinga, 2002) within our mesocosm, it is possible that a decrease in pH to values as low as pH 6.0 and 6.5 may have indirectly impacted the microbial activity. For example, during the CO_2 release experiment in Ardmucknish Bay, there was increased dissolution of minerals, including several toxic species (Lichtschlag et al. manuscript under review) and this was thought to have caused a decrease in the abundance of microbial 16S rRNA genes (Tait et al. 2015). For the diatom species, silicon biomineralisation may also be problematic within low pH environments (Hervé et al. 2012).

There is a need to understand the impacts of a CO_2 leak on the surrounding environment. In addition, the European Commission (EC) directive (2009/31/EC) on geological storage of CO_2 requires the establishment of a framework for the detection of CO_2 seep. An increased understanding of the possible scenarios triggered by CO_2 leaks could lead to low-cost strategies for monitoring CO_2. The QICS project concluded that the use of autonomous underwater vehicles equipped with a range of sensors, including both chemical and acoustic (for gas bubbles) would be a useful monitoring strategy (Blackford et al, 2014). Monitoring for blooms of microphytobenthos may also prove to be a low-cost, additional indicator of a CO_2 leak from injection pipeline failure in coastal areas. Along with direct observation, this could be monitored via chlorophyll pigment analysis of surface sediments. However, it is essential that these approaches are applied in conjunction with detailed, seasonal, baseline studies of potential CO_2 storage sites to determine natural variability in both the biology, but also natural variability in CO_2 levels. In addition, continued

comparisons to a nearby reference site of similar sediment characteristic and water depth would also be essential to untangle natural, temporal (both seasonal and diurnal) changes to the microphytobenthos community from those caused by CO_2 leakage.

Conclusions

The current study has demonstrated a clear impact to the microbial community, specifically an increase to primary producers, creating a visible bloom of *Spirulina* and diatom species. However although two diatom species dominated the surface sediment microbial communities, only one species, most closely related to a *Navicula* sp. also increased in abundance within the pH 7.0 treatments. More studies are required to understand the underlying mechanisms in the response of benthic *Cyanobacteria* and micro-algae to elevated levels of CO_2, including the possible role of carbon concentrating mechanisms and differences in sensitivities to pH. The microphytobenthos bloom did not occur within the pH 6.0 or 6.5 treatments and again more study is required to understand why this ~~is~~ occurred. Possibilities include increased grazing by meiobenthos, the release of toxic metals, as indicated by the Ardmucknish Bay field experiment (Licthschlag et al. manuscript under review), impacts to silicon biomineralisation or combinations of all of these factors. The abundance of photosynthetic microbes could prove to be an effective biological indicator for the detection and monitoring of CO_2 leaks within specific locations, such as pipelines within coastal areas.

Acknowledgements

The molecular characterisation of the microbial communities was supported through PML internal Research Project funding (PML RP) and we are grateful to Roche for the generous loan of a 454 GS Flx sequencer and materials required for both the preparation and sequencing of samples used in this study. The setting up and running of the mesocosm was funded by the European Project RISCS (European Community's Seventh Framework Programme (FP7/2007-2013) under grant agreement no. EU FP7 240837. HSF was in receipt of Lord Kingsland PML Fellowship. Thanks to the crew of Quest for collecting the sediment, Malcolm Woodward for overseeing the nutrient analysis and to Paul Somerfield for guidance on statistical analysis.

References

Atamanchuk D, Tengberg A, Aleynik D, Fietzek P, Hall POJ, Shitashima K & Stahl H (2015) Field-testing of methods and strategies to detect CO_2 leakage from a simulated sub-seabed storage site. *Int J Greenh Gas Control* In Press.

Beaufort L, Probert I, de-Garidel-Thoron T, Bendriff EM, Ruiz-Pino D, Metzl N, Goyet C, Buchet N, Coupel P, Grelaud M, Rost B, Rickaby REM & de Varges C (2011) Sensitivity of coccolithophores to carbonate chemistry and ocean acidification. *Nature* 476: 80-83.

Beman JM, Chow CE, King AL, Feng Y, Fuhrman JA, Andersson A, Bates NR, Popp BN & Hutchins D (2011) Global declines in oceanic nitrification rates as a consequence of ocean acidification. *Proc Nat Acad Sci USA* 108: 208-213.

Birks HJB, Line JM, Juggins S, Stevenson AC & Ter Braak CJF (1990) Diatoms and pH reconstruction. *Philos T R Soc A*, 327: 263-278.

Blackford JC, Jones N, Proctor R & Holt J (2008) Regional scale impacts of distinct CO_2 additions in the North Sea. *Mar Pollut Bull* 56: 1461–1468.

Blackford JC, Jones N, Proctor R, Holt J, Widdicombe S, Lowe D & Rees A (2009) An initial assessment of the potential environmental impact of CO_2 escape from marine carbon capture and storage systems. *Proc Inst Mech Eng A: J Power Energy* 223: 269–280.

Blackford JC, Stahl H, Bull JM, Bergès BJP, Cevatoglu M, Lichtschlag, A. et al. (2014) Detection and impacts of leakage from sub-seafloor Carbon Dioxide Storage. *Nature Climate Change* 4: 1011–1016.

Brewer PG & Riley JP (1965) The automatic determination of nitrate in seawater. *Deep Sea Res* 12: 765–772.

Burkhardt S, Amoroso F, Riebesell U & Sültemeyer DU (2001) CO_2 and HCO_3^- uptake in marine diatoms acclimated to different CO_2 concentrations. *Limnol Oceanogr* 46: 1378–1391.

Caporaso JG, Kuczynski J, Stombaugh J, Bittinger K, Bushman FD, Costello EK et al (2010) QIIME allows analysis of high-throughput community sequencing data. *Nature Methods* 7: 335-336.

Clarke KR & Gorley RN (2006) PRIMER v6: User Manual/Tutorial. PRIMER-E: Plymouth, UK.

Coolen MJL, Abbas B, van Bleijswijk J, Hopmans EC, Kuypers MMM, Wakeman SG & Sinninge Damsté JS (2007) Putative ammonia-oxidizing Crenarchaeota in suboxic waters of the Black Sea: a basin-wide ecological study using 16S ribosomal and functional genes and membrane lipids. *Environ Microbiol* 9: 1001-1016.

da Rosa APC, Carvalho LF, Goldbeck L, Costa JAV (2011) Carbon dioxide fixation by microalgae cultivated in open bioreactors. *Energy Conversion and Management* 52: 3071-3073.

582 Dickson AG & Millero FJ (1987) A comparison of the equilibrium constants for the dissociation of
583 carbonic-acid in seawater media. *Deep-Sea Res* 34: 1733-1743.
584 Dickson AG (1990) Thermodynamics of the dissociation of boric acid in potassium-chloride solutions
585 form 273.15 K to 318.15 K. *J Chem Thermodyn* 22: 113-127.
586 Dickson AG, Sabine CL & Christian JR (2007) Guide to best practices for ocean CO_2 measurements.
587 PICES special publication, 3.
588 Erguder TH, Boon N, Wittebolle L, Marzorati M & Verstraete W (2009) Environmental factors shaping
589 the ecological niches of ammonia-oxidizing archaea. *FEMS Microbiol Rev* 33: 855-869.
590 Findlay HS, Kendall MA, Spicer JI & Widdicombe S (2010) Relative influences of ocean acidification
591 and temperature on intertidal barnacle post-larvae at the northern edge of their geographic
592 distribution. *Estuar Coast Shelf Sci* 86: 675-682.
593 Franks J & Stolz JF (2009) Flat laminated microbial mat communities. *Earth Sci Rev* 96: 163-172.
594 Fu FX, Mulholland MR, Garcia NS, Beck A, Bernhardt PW, Warner ME, Sañudo-Wihelmy SA &
595 Hutchins DA (2008) Interactions between changing pCO_2, N_2 fixation, and Fe limitation in the
596 marine unicellular cyanobacterium *Crocosphaera*. *Limnol Oceanogr* 53: 2472–2484.
597 Global CCS Institute (2012) Global status of CCS.
598 http://www.globalccsinstitute.com/publications/global-status-ccs-2012
599 Grasshoff K (1976) Methods of Seawater Analysis. Verlag Chemie, Weiheim.
600 Hartikainen H, Pitkänen M, Kairesalo T & Tuominen L (1996) Co-occurrence and potential chemical
601 competition of phosphorus and silicon in lake sediment. *Water Research* 30: 2472-2478.
602 Håvelsrud OE, Haverkamp TH, Kristensen T, Jakobsen KS & Rike AG (2012) Metagenomic and
603 geochemical characterization of pockmarked sediments overlaying the Troll petroleum
604 reservoir in the North Sea. *BMC Microbiol* 12, 203.
605 Håvelsrud OE, Haverkamp TH, Kristensen T, Jakobsen KS & Rike AG (2013) Metagenomics in CO_2
606 monitoring. *Energy Procedia* 37, 4215-4233.
607 Hervé V, Derr J, Douady S, Quinet M, Moisan L & Lopez PJ (2012) Multiparametric Analyses Reveal
608 the pH-Dependence of Silicon Biomineralization in Diatoms. *PloS One* 7: e46722.
609 Hinga KR (2002) Effects of pH on coastal marine phytoplankton. *Mar Ecol Prog Ser* 238: 280-300.
610 Holloway S (2007) Carbon dioxide capture and geological storage. *Philos T R Soc A* 365: 1095-1107.
611 Hopkinson BM, Dupont CL, Allen AE & Morel FM (2011) Efficiency of the CO_2-concentrating
612 mechanism of diatoms. *P Natl Acad Sci* 108: 3830-3837.
613 Hubas C, Jesus B, Passarelli C & Jeanthon C (2011) Tools providing new insight into coastal
614 anoxygenic purple bacterial mats: review and perspectives. *Res microbiol* 162: 858-868.

Huse SM, Welch DM, Morrison HG & Sogin ML (2010) Ironing out the wrinkles in the rare biosphere through improved OTU clustering. *Environ Microbiol* 12: 1889-1898.

Hutchins DA, Fu F, Zhang Y, Warner ME & Feng Y (2007) CO_2 control of *Trichodesmium* N_2 fixation, photosynthesis, growth rates, and elemental ratios: Implications for past, present, & future ocean biogeochemistry. *Limonol Oceanogr* 52: 1293-1304.

Ishida H, Watanabe Y, Fukuhara T, Kaneko S, Furusawa K & Shirayama Y (2005) In situ enclosure experiment using benthic chamber system to assess the effect of high concentration of CO_2 on deep-sea benthic communities. *J Oceanogr* 61: 835–843.

Ishida H, Gomen LG, West J, Krüger M, Coombs P, Berge JA, Fukuhara T, Magi M & Kita J (2013) Effects of CO_2 on benthic biota: An *in situ* benthic chamber experiment in Storfjorden (Norway). *Mar Pollut Bull* 73: 443-51.

Kerfahi D, Hall-Spencer JM, Tripathi BM, Milazzo M, Lee J & Adams JM (2014) Shallow water marine sediment bacterial community shifts along a natural CO_2 gradient in the Mediterranean Sea off Vulcano, Italy. *Microb Eco* 67: 819-828.

Kim JM, Lee K, Shin K, Shin K, Kang JH, Lee HW, Kim M, Jang PG, Jang MC (2006) The effect of seawater CO_2 concentration on growth of a natural phytoplankton assemblage in a controlled mesocosm experiment. *Limnol Oceanogr* 51: 1629–1636.

Kirkwood D (1989) Simultaneous determination of selected nutrients in seawater. International Council for the Exploration of the Sea (ICES), CM 1989/C:29.

Kitidis V, Laverock B, McNeil CL, Beesley A, Cummings D, Tait K, Osborn AM, Widdicombe S (2011) The impact of ocean acidification on sediment nitrification. *Geophysical Research Letters*. doi:10.1029/2011GL049095.

Komárek J, Hauer T (2010) CyanoDB. cz–on-line database of cyanobacterial genera. World-Wide Electronic Publication, University of South Bohemia & Institute of Botany AS CR.

Langer G, Nehrke G, Probert I, Ly J, Ziveri P (2009) Strain-specific responses of *Emiliania huxleyi* to changing seawater carbonate chemistry. *Biogeosci Discuss* 6: 4361–4383.

Levitan O, Brown C, Sudhaus S, Campbell DA, LaRoche J, Berman-Frank I (2010) Regulation of nitrogen metabolism in the marine diazotroph *Trichodesmium* IMS101 under varying temperatures and atmospheric CO2 concentrations. *Environ Microbiol* 12: 1899−1912.

Lichtschlag A, James RH, Stahl H & Connelly D (2015) Effect of a controlled sub-seabed release of CO2 on the biogeochemistry of shallow marine sediments, their pore waters, and the overlying water column. *Int J Greenh Gas Control* In Press.

Mantoura RFC & Woodward EMS (1983) Optimization of the indophenol blue method for the automated determination of ammonia in estuarine waters. *Estuar Coast Shelf Sci* 17: 219–224.

Mehrbach C, Culberson CH, Hawley JE & Pytkowicz RM (1973) Measurements of the apparent dissociation constants of carbonic acid in seawater at atmospheric pressure. *Limnol Oceanogr* 18: 897–907.

Metz B, Davidson O, De Coninck H, Loos M & Meyer L (2005) IPCC special report on carbon dioxide capture and storage. Intergovernmental Panel on Climate Change, Geneva (Switzerland). Working Group III.

Middleburg JJ, Barranguet C, Boschker HT, Herman PM, Moens T & Heip CH (2000) The fate of intertidal microphytobenthos carbon: An in situ 13C-labeling study. *Limnol Oceanogr* 45: 1224-1234.

Miller DC, Geider RJ & MacIntyre HL (1996) Microphytobenthos: the ecological role of the "secret garden" of unvegetated, shallow-water marine habitats. II. Role in sediment stability and shallow-water food webs. *Estuar Coast* 19: 202-212.

~~Mohamed NM, Saito K, Tal Y & Hill RT (2010) Diversity of aerobic and anaerobic ammonia-oxidizing bacteria in marine sponges. *ISME J* 4: 38-48.~~

Nübel U, Garcia-Pichel F & Muyzer G (1997) PCR primers to amplify 16S rRNA genes from cyanobacteria. Appl *Environ Microbiol* 63: 3327-32.

Paterson DM & Hagerthey SE (2001) Microphytobenthos in constrasting coastal ecosystems: biology and dynamics. In Reise K (eds) Ecological comparisons of sedimentary shores. Ecological studies vol. 151. Springer Verlag p 105-125.

Pierrot D, Lewis E & Wallace DWR (2006) CO2sys DOS program developed for CO_2 system calculations. ORNL/CDIAC-105. Carbon Dioxide Information Analysis Centre, Oak Ridge National Laboratory, U.S. Department of Energy, Oak Ridge, Tennessee.

Pruesse E, Quast C, Knittel K, Fuchs BM, Ludwig W, Peplies J & Glöckner FO (2007) SILVA: a comprehensive online resource for quality checked and aligned ribosomal RNA sequence data compatible with ARB. *Nucl Acids Res* 35: 7188-7196.

Quince C, Lanzen A, Davenport RJ & Turnbaugh PJ (2011) Removing noise from pyrosequenced amplicons. *BMC bioinformatics* 12: 38.

Ramanan R, Kannan K, Deshkar A, Yadav R & Chakrabarti T (2010) Enhanced algal CO_2 sequestration through calcite deposition by *Chlorella* sp. and *Spirulina platensis* in a mini-raceway pond. *Bioresour Technol* 101: 2616-2622.

Rappe MS, Kemp PF & Giovannoni SJ (1997) Phylogenetic diversity of marine coastal picoplankton 16S rRNA genes cloned from the continental shelf off Cape Hatteras, North Carolina. *Limnol Oceanogr* 42: 811-826.

Raven JA (1991) Physiology of inorganic C acquisition and implications for resource use efficiency by marine phytoplankton: relation to increased CO_2 and temperature. *Plant Cell Environ* 14: 779–794.

Reinfeilder JR (2011) Carbon concentrating mechanisms in Eukaryotic marine phytoplankton. *Annu Rev Mar Sci* 3:291–315.

Rost B, Riebesell U, Burkhardt S & Sültemeyer D (2003) Carbon acquisition of bloom forming marine phytoplankton. *Limnol Oceanogr* 48: 55–67.

Russell BD, Connell SD, Findlay HS, Tait K, Widdicombe S & Mieszkowska N. (2013) Ocean acidification and rising temperatures may increase biofilm primary productivity but decrease grazer consumption. *Philos T R Soc B*. 368(1627): 20120438.

Smith CJ, Nedwell DB, Dong LF & Osborn AM (2006) Evaluation of quantitative polymerase chain reaction-based approaches for determining gene copy and gene transcript numbers in environmental samples. *Environ Microbiol* 8: 804-815.

Stumpp M, Trübenbach K, Brennecke D, Hu MY & Melzner F (2012) Resource allocation and extracellular acid-base status in the sea urchin *Strongylocentrotus droebachiensis* in response to CO2 induced seawater acidification. *Aqu Toxicol* 110-111: 194-207.

Sun J, Hutchins DA, Feng Y, Seubert EL, Caron DA & Fu FX (2011) Effects of changing pCO_2 and phosphate availability on domoic acid production and physiology of the marine harmful bloom diatom *Pseudo-nitzschia* multi-series. *Limnol Oceanogr* 56: 829-840.

Tait K, Laverock B, Shaw J, Somerfield PJ & Widdicombe S (2013) Minor impact of ocean acidification to the structure of the active microbial community in an Arctic sediment. *Env Microbiol Rep* 5, 851-860.

Tait K, Stahl S, Taylor P & Widdicombe S (2015) Rapid response of the active microbial community to CO_2 exposure from a controlled sub-seabed CO_2 leak in Ardmucknish Bay (Oban, Scotland). *Int J Greenh Gas Control* In Press.

Tamura K, Dudley J, Nei M & Kumar S (2007) MEGA4: Molecular Evolutionary Genetics Analysis (MEGA) software version 4.0. *Mol Biol Evol* 24:1596-1599.

Taylor JD, Ellis R, Milazzo M, Hall-Spencer JM & Cunliffe (2014) Intertidal epilithic bacteria diversity changes along a naturally occurring carbon dioxide and pH gradient. *FEMS Microbiol Ecol* 89: 670-678.

Taylor P, Stahl H, Blackford J, Vardy ME, Bull JM, Akhurst M, Hauton C, James RH, Lichtschlag A, Long D, Aleynik D, Toberman M, Naylor M, Connelly D, Smith D, Sayer DJ, Widdicombe S & Wright IC (2015a) Introduction to a novel in situ sub-seabed CO_2 release experiment for quantifying and monitoring potential ecosystem impacts from geological carbon storage. *Int J Greenh Gas Control* In Press.

Taylor P, Lichtschlag A, Toberman M, Sayer MDJ, Reynolds A, Sato T & Stahl H (2015b) Impact and recovery of pH in marine sediments subject to a temporary carbon dioxide leak. *Int J Greenh Gas Control* In Press.

Thomsen J, Casties I, Pansch C, Körtzinger A & Melzner F. (2013) Food availability outweighs ocean acidification effects in juvenile *Mytilus edulis*: laboratory and field experiments. *Global Change Biology* 19: 1017–1027.

Torstensson A, Chierici M & Wulff A (2012) The influence of increased temperature and carbon dioxide levels on the benthic/sea ice diatom *Navicula directa*. *Polar Biol* 35: 205-214.

Tortell PD, Payne CD, Li YH, Trimborn S, Rost B, Smith WO, Riesselman C, Dunbar RB, Sedwick P & DiTullio GR (2008) CO_2 sensitivity of Southern Ocean phytoplankton. *Geophys Res Lett* 35, L04605, doi:10.1029/2007GL032583.

Trimborn S, Wolf-Gladrow D, Richter KU & Rost B (2009). The effect of pCO_2 on carbon acquisition and intracellular assimilation in four marine diatoms. J Exp Mar Biol *Ecol* 376: 26-36.

Underwood GJC & Kromkamp J (1999) Primary production by phytoplankton and microphytobenthos in estuaries. *Adv Ecol Res* 29: 93-153.

Widdicombe S & Needham HR (2007) Impact of CO_2-induced seawater acidification on the burrowing activity of *Nereis virens* and sediment nutrient flux. *Mar Ecol Prog Ser* 341: 111–122.

Yanagawa K, Morono Y, de Beer D, Haeckel M, Sunamura M, Futagami T, Hoshino T, Terada T, Nakamura K, Urabe T, Rehder G, Boetius A & Inagaki F (2012) Metabolically active microbial communities in marine sediment under high-CO2 and low-pH extremes. *ISME J* 7: 555-567.

Zhang JZ & Chi J (2002) Automated analysis of nanomolar concentrations of phosphate in natural waters with liquid waveguide. *Environ Sci Technol* 36: 1048–1053.

Table 1: Environmental conditions in the cores averaged over the 10 week experimental period, values are means (± 95 % confidence intervals). pH, temperature (ºC), salinity and total alkalinity (TA, µmol kg^{-1}) were measured and used to calculate pCO_2 (µatm), dissolved inorganic carbon (DIC, µmol kg^{-1}), and saturation states for calcite (Ω_C) and aragonite (Ω_A). Also shown are average water nutrient concentrations (µM) calculated from measurements taken throughout the 10 week incubation period.

target pH	8.0	7.5	7.0	6.5	6.0
pH	7.98 (± 0.021)	7.47 (± 0.043)	7.11 (± 0.032)	6.69 (± 0.032)	6.14 (± 0.030)
Temperature (°C)	10.8 (± 0.08)	11.0 (± 0.12)	11.1 (± 0.14)	10.8 (± 0.07)	10.6 (± 0.09)
Salinity	33.8 (± 0.10)	33.7 (± 0.08)	33.7 (± 0.07)	33.8 (± 0.08)	33.7 (± 0.07)
TA (µmol kg^{-1})	2561 (± 50)	2512 (± 49)	2531 (± 53)	2572 (± 39)	2594 (± 83)
pCO_2 (µatm)	711 (± 25)	2382 (± 190)	5627 (± 309)	15157 (± 924)	54396 (± 1902)
DIC (µmol kg^{-1})	2441 (± 40)	2564 (± 35)	2748 (± 38)	3214 (± 30)	4937 (± 52)
Ω_C	2.52 (± 0.16)	0.84 (± 0.10)	0.37 (± 0.04)	0.14 (± 0.02)	0.04 (± 0.01)
Ω_A	1.6 (± 0.11)	0.53 (± 0.07)	0.24 (± 0.02)	0.09 (± 0.01)	0.03 (± 0.01)
Ammonia	0.85 (± 0.33)	0.75 (± 0.27)	0.55 (± 0.13)	0.70 (± 0.4)	0.85 (± 0.21)
Nitrate	6.15 (± 1.01)	6.51 (± 1.18)	6.93 (± 0.94)	5.96 (± 0.97)	6.33 (± 0.93)
Nitrite	0.14 (± 0.018)	0.14 (± 0.021)	0.13 (± 0.019)	0.10 (± 0.013)	0.15 (± 0.027)
Phosphate	0.55 (± 0.09)	0.64 (± 0.16)	0.63 (± 0.12)	0.68 (± 0.11)	0.69 (± 0.11)
Silicate	5.25 (± 0.41	5.20 (± 0.54)	5.13 (± 0.38)	5.38 (± 0.44)	5.27 (± 0.42)

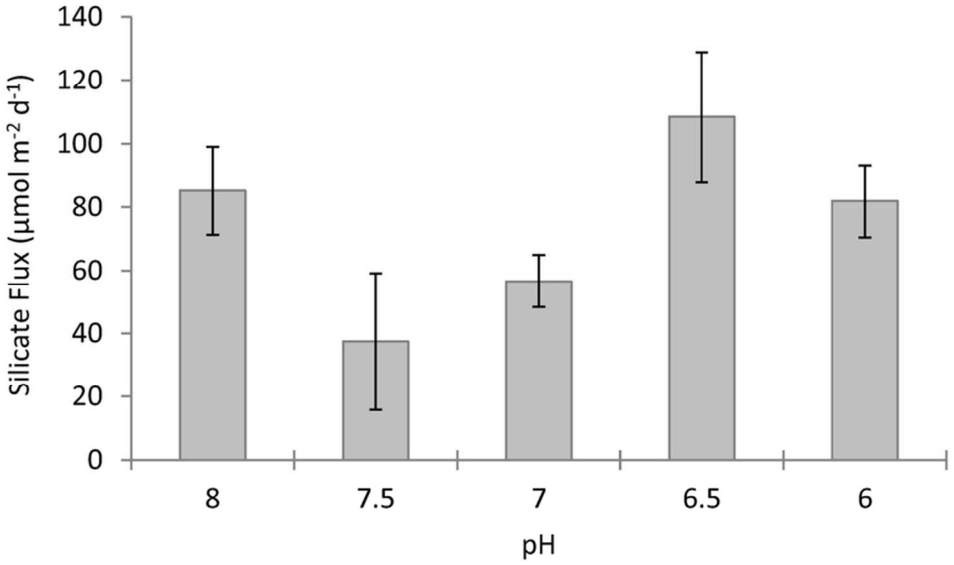

Impact of seawater pH on average silicate flux rates. Error bars are standard deviation (n = 5).
76x45mm (300 x 300 DPI)

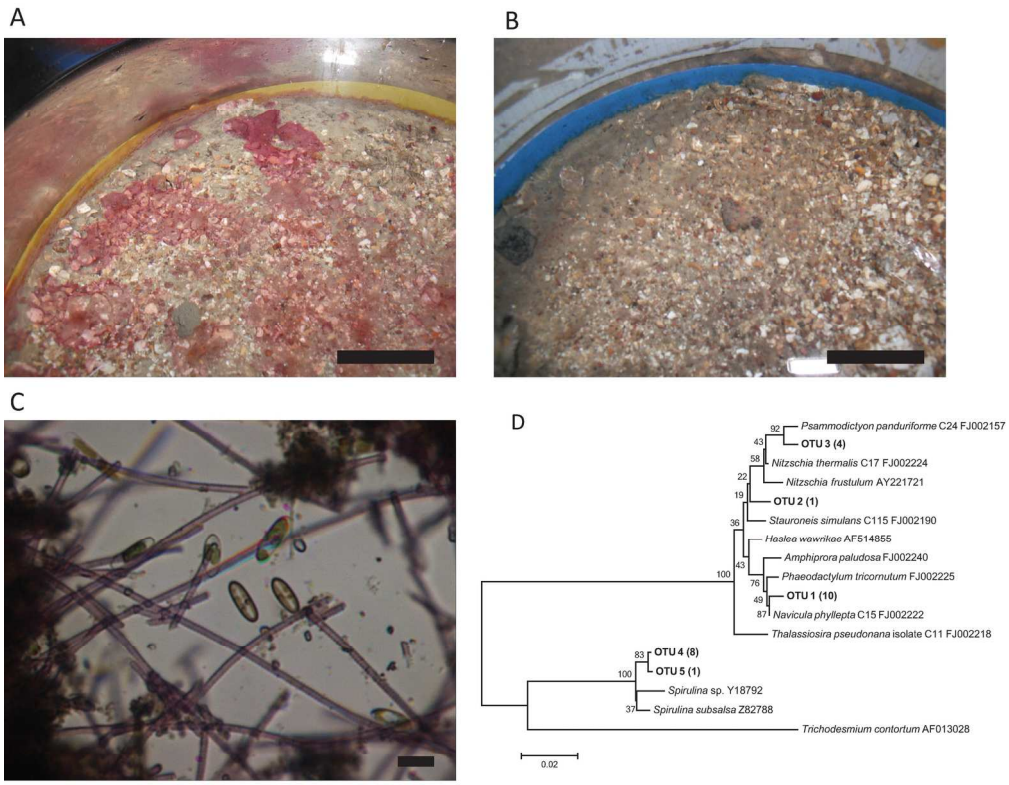

Comparison of sediment surface of cores incubated at pH 7.0 (A) and pH 8.0 (B). A pink mat of microphytobenthos mat can be clearly seen in the cores exposed to pH 7.0. Bar is 3 cm. (C) Microscope image of microphytobenthos mat showing the presence of pink cyanobacterial filaments and diatoms. Bar is 100 µm. (D) Phylogenetic tree of Cyanobacterial and Chloroplast 16S rRNA OTU data derived from clone libraries of segments of the pink microphytobenthos mat calculated using MEGA 5 (Tamura et al., 2007). OTUs were identified at 97% nucleotide similarity. The number of sequences found within each OTU is indicated in brackets. The tree topology is based on maximum likelihood and bootstrap analysis was performed with 1000 replications (MEGA 5). Reference sequences and their accession numbers are also shown
171x165mm (300 x 300 DPI)

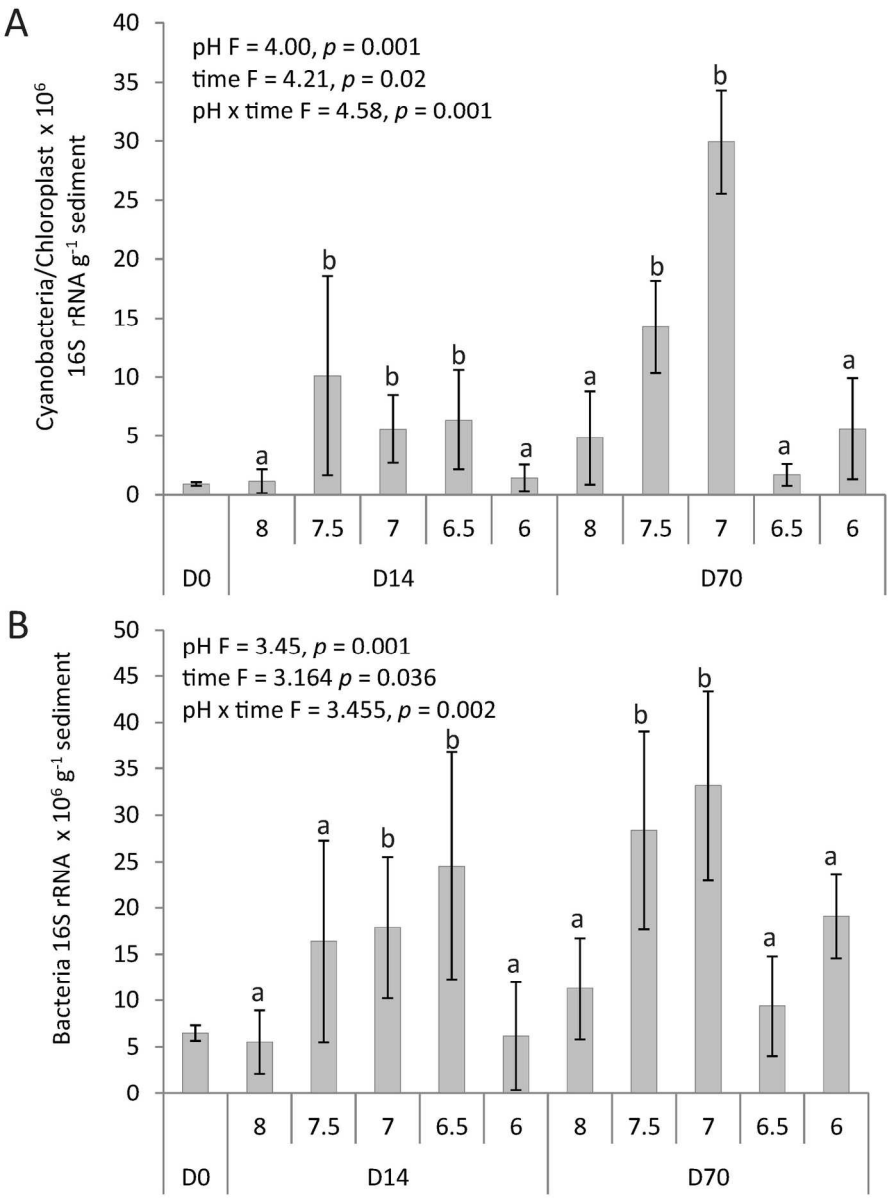

Effect of pH on the abundance of cyanobacterial/micro-algal 16S rRNA (g-1 sediment. For each pH, five separate cores were used. The results of PEMANOVA tests for significant difference between pH treatments and week sampled are shown above each graph. Statistical differences between all treatments are indicated by asterisks: ***p ≤0.001, **p ≤0.01, *p ≤0.05; significant differences (p ≤0.05) between individual treatments are indicated by different letters. Error bars are standard deviation (n = 5).

158x208mm (300 x 300 DPI)

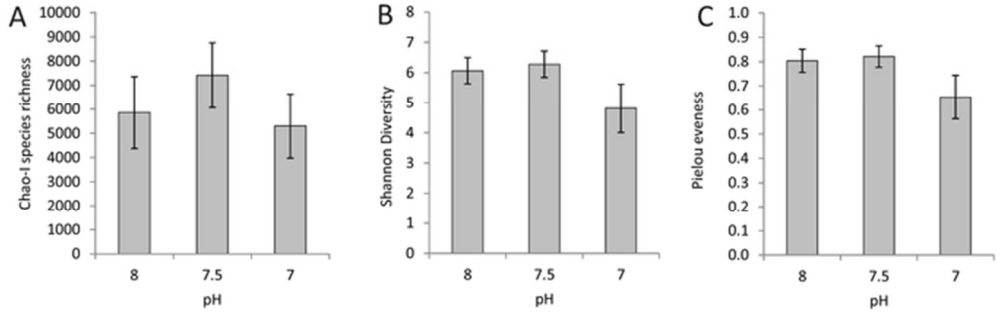

Effect of pH on measurements of alpha diversity including (A) Chao-I species richness, (B) Shannon diversity and (C) Pielou eveness. Error bars are standard deviation (n = 5).
57x18mm (300 x 300 DPI)

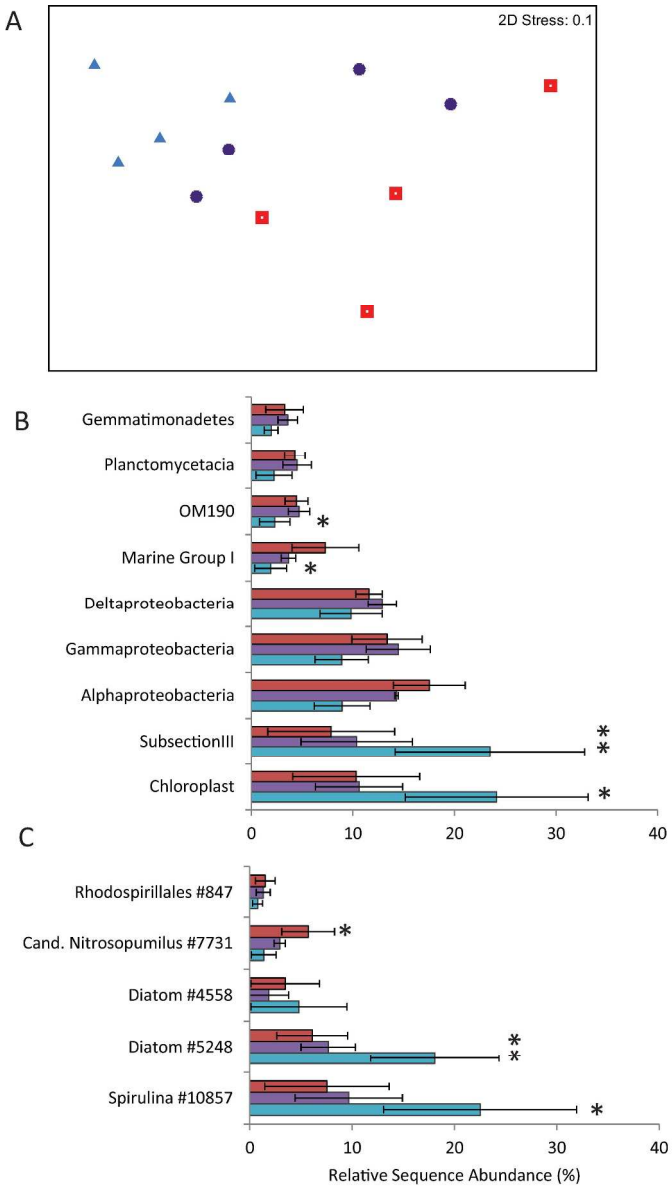

The effect of pH on microbial community composition including (A) Non-metric multidimensional scaling (MDS) ordination of a Bray–Curtis resemblance matrix (red open squares are pH 8.0, purple asterisks are pH 7.5 and blue closed triangles pH 7.0), and the effect of pH on (A) the abundance of the microbial classes with abundances > than 2%, and (B) the top five most abundant OTUs. Blue bars are pH 7.0, purple bars are pH 7.5 and red bars are pH 8.0 treatments. Significant differences when compared to pH 8.0 treatments at each time point are indicated by ** for $p \leq 0.01$ and * for $p \leq 0.05$. Error bars are standard deviation (n = 5).
229x403mm (300 x 300 DPI)

Supplementary Table 1: Comparison of sequence data from each core and CO_2 treatment. Shown are the number of sequences per sample post-processing, the number of OTUs (clustered at 97% sequence similarity) and the ratio of bacterial:archaeal sequences in the data-set. This is compared to the ratio of bacteria:archaea obtained by RT qPCR of 16S rRNA. Due to the variability amongst the numbers of sequences obtained for each sample, all cores were sub-sampled to the lowest value, 5237 (obtained for core no. 28). Also shown (in bold) are totals calculated from combined sequence data from each CO_2 treatment.

		RAW DATA				RE-SAMPLED DATA (5237 sequences per core) - 97% similarity	
pH	Core Number	No. sequences	No. OTUs	Ratio Archaeal: Bacterial sequences	Ratio Archaea: Bacteria qPCR	No. OTUs	Ratio Archaeal: Bacterial sequences
8	26	7490	3482	0.05	0.04	1916	0.05
	27	7002	2794	0.11	0.11	1686	0.11
	28	5237	2664	0.07	0.08	1861	0.07
	29	8843	4629	0.12	0.18	2118	0.13
	TOTAL	**28572**	**13406**	**0.09**	**0.10**	**5630**	**0.09**
7.5	31	9869	4205	0.03	0.03	1963	0.03
	32	10292	4025	0.04	0.09	1789	0.05
	33	10109	5143	0.07	0.09	2307	0.07
	35	11535	6257	0.04	0.07	2288	0.04
	TOTAL	**41805**	**19403**	**0.05**	**0.07**	**6442**	**0.05**
7	37	10712	4594	0.01	0.04	2052	0.01
	38	6870	2312	0.10	0.08	1395	0.10
	39	6199	1943	0.03	0.05	1335	0.03
	40	15424	4425	0.01	0.04	1485	0.01
	TOTAL	**39205**	**13162**	**0.04**	**0.05**	**4931**	**0.04**